J. Hydrol. Hydromech., 62, 2014, 2, 150–159
DOI: 10.2478/johh-2014-0013

Numerical and physical model study of a vertical slot fishway

Martin Bombač[1*], Gorazd Novak[1], Primož Rodič[1], Matjaž Četina[2]

[1] Institute for Hydraulic Research, Hajdrihova 28, 1000, Ljubljana, Slovenia. E-mails: gorazd.novak@hidroinstitut.si; primoz.rodic@hidroinstitut.si
[2] Chair of Fluid Mechanics with Laboratory, Faculty of Civil and Geodetic Engineering, University of Ljubljana, Hajdrihova 28, 1000, Ljubljana, Slovenia. E-mail: matjaz.cetina@fgg.uni-lj.si
[*] Corresponding author. E-mail: martin.bombac@hidroinstitut.si

Abstract: This paper presents the results of an experimental and numerical study of a vertical slot fishway (VSF). A 2-D depth-averaged shallow water numerical model PCFLOW2D coupled with three different turbulent models (constant eddy viscosity, Smagorinsky and $k - \varepsilon$) was used. A detailed analysis of numerical parameters needed for a correct simulation of the phenomenon was carried out. Besides the velocity field, attention was paid to important hydraulic parameters such as maximum velocity in the slot region and energy dissipation rate ε in order to evaluate the performance of VSF. A scaled physical hydraulic model was built to ensure reliable experimental data for the validation of the numerical model. Simulations of variant configurations of VSF showed that even small changes in geometry can produce more fish-friendly flow characteristics in pools. The present study indicates that the PCFLOW2D program is an appropriate tool to meet the main demands of the VSF design.

Keywords: Eddy viscosity; Hydraulic model; Numerical diffusion; Numerical model PCFLOW2D; Turbulence model; Vertical slot fishway.

INTRODUCTION

The result of the construction and impoundment of a river with a hydropower plant (HPP) is the interruption of fish migration routes. The purpose of migration is to reach suitable spawning areas, find food, avoid adverse conditions (high or low temperature), or simply to spread the habitat of certain species. Individual habitats, where fish meet the needs in a given period of their life cycle, can be widely separated (HESS, 2010). Fish need to be able to get over such obstacles in both directions for a successful life cycle. Fishways are hydraulic structures that enable the passage of fish under all circumstances and for all the species concerned, and therefore play a vital ecological role (Violeau, 2012). They are designed to attract fish readily and allow them to enter, pass through and exit safely with no undue stress, injury and especially without any undue delay for adult spawners (Liu et al., 2006).

The EU Water Framework Directive adopted in 2000 obligates Slovenia to smooth the way for water organisms to migrate. In Slovenia, fish passages are now legally obligatory for all newly constructed power plants while existing plants are to be either equipped with fish passages, or the currently non-functional passages are to be renewed, depending on the interests of power production concessionaires and on the implementation of the EU Water Framework Directive demands for improved ecological condition of watercourses (Kolman et al., 2010). The present study presents a reliable tool for a detailed determination of flow structures in fishway pools and should prove useful in the process of VSF design.

A vertical slot fishway (VSF) is a channel divided into several pools separated by slots. For uniform flow conditions, the flow pattern in a vertical slot fishway depends mainly on the specific pool design, i.e. geometry of the pool (Puertas et al., 2004; Rajaratnam et al., 1992). Once a suitable pool design has been found, a vertical slot fishway will work effectively for a wide range of discharges (Clay, 1995) because the flow pattern is relatively insensitive to variations of the total flow (Cea et al., 2007). The flow pattern in the pools is of great importance in order to guide the fish through the fishway. The velocity field and water depth in the pool affect the swimming costs of fish and the turbulence level has proved to increment it considerably (Clay, 1995; Enders et al., 2003; Powers and Orsborn, 1984).

Several experimental studies of the flow field in vertical slot fishways showed that the flow in the major part of the pool is almost two-dimensional (2-D), with small vertical velocities relative to the horizontal ones (Liu et al., 2006; Pena et al., 2004; Puertas et al., 2004; Rajaratnam et al., 1986; Tarrade et al., 2008; Wu et al., 1999). Larger vertical velocities may occur only in the slot region and depend mainly on the slope of the fishway, more precisely on the difference in water levels between two adjacent pools. The observation, that the flow in VSF is mostly 2-D in nature, opens up the possibility of using a depth-averaged shallow water model in order to compute the flow field in VSF (Cea et al., 2007). Previous numerical studies by Cea et al. (2007), Chorda et al. (2010) and Violeau (2012) have used this approach to study flow characteristics such as velocities, water surface elevations, local vorticity, turbulent kinetic energy per unit mass k, and energy dissipation rate per unit mass ε. Their numerical results were in accordance with experimental data and thus confirmed the appropriateness of such numerical models.

The objective of this paper is twofold. The first aim was to verify the possibility of using a 2-D mathematical model PCFLOW2D that has been developed (and is continuously being improved) at the Chair of Fluid Mechanics with Laboratory, Faculty of Civil and Geodetic Engineering, University of Ljubljana to simulate Newtonian (Četina, 1988; Četina, 2000; Hamzić, 2012) and non-Newtonian free surface flows (Četina et al., 2006) for correct determination of flow field and other hydraulic parameters in VSF. Second, the influence of turbulence and its proper modelling in the VSF was investigated. Sensitivity analysis of the numerical mesh used in the mathematical model demonstrates the phenomena of numerical diffusion. The case study is a VSF at HPP Blanca which was built in 2007 and is at present the only functional fishway in Slovenia

(Kolman et al., 2010). A scaled physical hydraulic model was built to provide reliable experimental data for the validation of the numerical model. Numerical model PCFLOW2D is equipped with three different turbulent models: constant eddy viscosity, Smagorinsky and $k - \varepsilon$. A detailed analysis of numerical parameters needed for the proper simulation of the phenomenon was carried out. Simulations of variant configurations of VSF Blanca were made. It was shown that even small changes in geometry can produce more fish-friendly flow characteristics in pools.

VERTICAL SLOT FISHWAY DESIGN

The upper part of the VSF at HPP Blanca is a 2.2 m wide channel with longitudinal slope S_0 = 1.67% and consists of 24 pools of length L = 3.0 m and slot width b_0 = 0.59 m (Josipovič and Ciuha, 2009). The numerical and physical models of the VSF consisted of 5 pools with L = 3.0 m, a 6.0 m long inlet reach (2 x L) and 9.0 m long outlet reach (3 x L) (Fig. 1). Such model dimensions ensure uniform flow past the central pools, with no potential effects of the model inlet and outlet boundary conditions (Chorda et al., 2010; Liu et al., 2006). Therefore, all detailed measurements and analyses were carried out in the third (middle) pool.

(a)

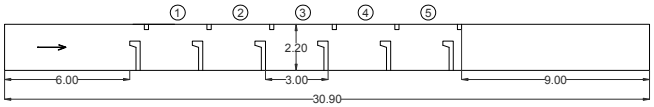

b)

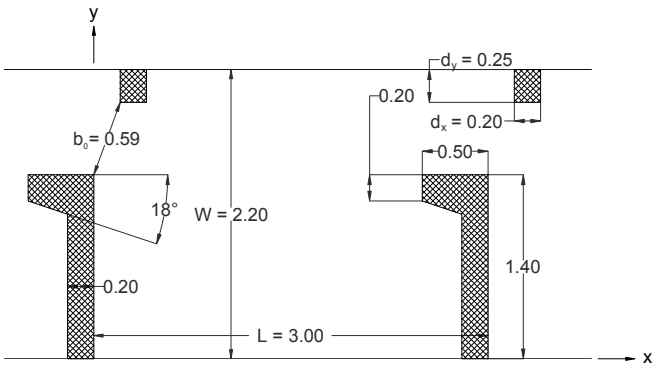

Fig. 1. Prototype geometry of VSF Blanca: (a) plan view, and (b) details of slot and pool. Dimensions are in meters.

EXPERIMENTAL SETUP

A 1:4.4 scale physical model was built at the Institute for Hydraulic Research, Ljubljana in a 0.5 m wide rectangular glass flume using Froude similitude. The model bed was made of plastic; baffles separating the pools were made of wood. The inflow discharge Q of 14.77 l/s (corresponding to 600 l/s for prototype) was measured with V-notch weir to ± 1.5%. Tailwater was regulated with an adjustable plate weir to reach uniform flow conditions in the VSF. Free surface elevations along the VSF were measured using a point gauge with ± 0.1 mm reading accuracy.

The velocity field in the central pool was measured with an ADV SonTek 2D-probe. ADV is partially flow-intrusive. Probe sampling volume was located 50 mm from the probe tip. Measuring range was set to 1 m/s with an accuracy of ± 1%. Sampling frequency was set to 25 Hz. Velocity components U_x (streamwise direction) and U_y (transverse direction) were measured in 4 cross sections located at x = 0.6, 1.2, 1.8 and 2.3 m from the beginning of the middle pool (Fig. 2). In each cross section, a total of 96 points were measured in 24 equally spaced verticals. Measurements were taken at 4 different depths: z = 0.05, 0.25, 0.45 and 0.65 m above bottom.

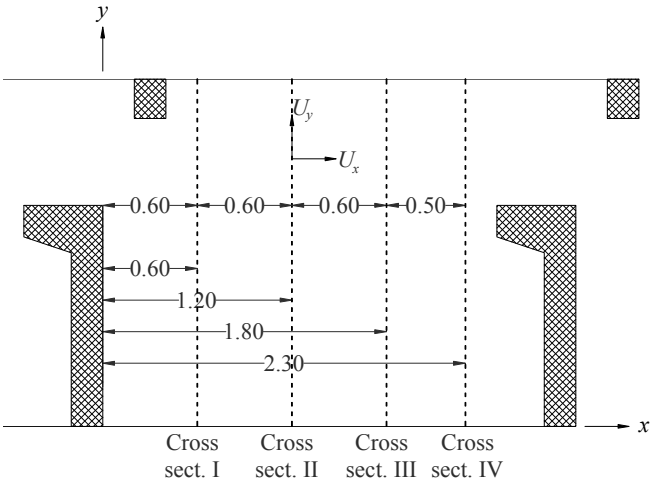

Fig. 2. Cross sections in central pool of VSF in which velocities were measured. Dimensions are in meters.

NUMERICAL MODEL

The numerical model PCFLOW2D (Četina, 1988; Četina, 2000; Hamzić, 2012) solves the depth-averaged shallow water equations coupled with a turbulence model. The 2-D depth-averaged shallow water equations can be written in conservative form as:

$$\frac{\partial h}{\partial t}+\frac{\partial\left(hu_x\right)}{\partial x}+\frac{\partial\left(hu_y\right)}{\partial y}=0\,, \tag{1}$$

$$\frac{\partial\left(hu_x\right)}{\partial t}+\frac{\partial\left(hu_x^2\right)}{\partial x}+\frac{\partial\left(hu_xu_y\right)}{\partial y}=-gh\frac{\partial h}{\partial x}-gh\frac{\partial z_b}{\partial x}-$$
$$-ghn_g^{\,2}\frac{u_x\sqrt{u_x^2+u_y^2}}{h^{\frac{4}{3}}}+\frac{\partial}{\partial x}\left(h\nu_T\frac{\partial u_x}{\partial x}\right)+\frac{\partial}{\partial y}\left(h\nu_T\frac{\partial u_x}{\partial y}\right), \tag{2}$$

$$\frac{\partial\left(hu_y\right)}{\partial t}+\frac{\partial\left(hu_xu_y\right)}{\partial x}+\frac{\partial\left(hu_y^2\right)}{\partial y}=-gh\frac{\partial h}{\partial y}-gh\frac{\partial z_b}{\partial y}-$$
$$-ghn_g^{\,2}\frac{u_y\sqrt{u_x^2+u_y^2}}{h^{4/3}}+\frac{\partial}{\partial x}\left(h\nu_T\frac{\partial u_y}{\partial x}\right)+\frac{\partial}{\partial y}\left(h\nu_T\frac{\partial u_y}{\partial y}\right)\,, \tag{3}$$

where h is the water depth; u_x and u_y are the depth-averaged velocities in x and y direction; g is the gravity acceleration; z_b is the bed elevation level; n_g is Manning's roughness coefficient and v_T is kinematic coefficient of eddy viscosity determined by the appropriate turbulence model.

The system of partial differential equations is solved through the Patankar-Spalding finite volume numerical method (Patankar, 1980). For spatial discretization the hybrid scheme (combination of central differences and upwind scheme depending on the cell Peclet's numbers P_e) is used. A fully implicit scheme is used for time integration. This scheme is stable

and sufficiently accurate even at longer time intervals and relatively high Courant numbers (Valentine et al., 2002). The iterative procedure of depth corrections known as SIMPLE is used in the model.

Description of model simulations

All simulations in the present study were done for constant discharge Q = 600 l/s. This discharge corresponded to 14.77 l/s in the 1:4.4 physical model. The presented experimental results of the physical model were scaled accordingly. Additionally, PCFLOW2D was employed to evaluate scale effects. Employing the same numerical settings (i.e. grid and other parameters) in two simulations of both the prototype and the physical model conditions gave results that were almost identical which proved there were no significant scale effects. Knowing that a fish-friendly flow analysis lies upon full scale values (Chorda et al., 2010) (fish length, burst speed, etc.) all results are presented at full scale.

Boundary and initial conditions

Boundary conditions of PCFLOW2D consisted of constant discharge with uniform discharge profile normal to the inlet boundary, and a depth-discharge relation at the outlet boundary. The depth-discharge relation was determined iteratively with a goal of obtaining the same water depth in middle sections of pools 2, 3 and 4 (uniform flow condition). This was achieved after several runs with constant value for the eddy viscosity v_T, and varying the outlet free surface elevation. In the present study, the outlet boundary condition was set at h_{out} = 0.88 m. Detailed results and comparisons focus was on the third pool, assuming that the effect of fishway inlet and outlet boundary conditions is minimal there. The wall velocity boundary condition takes into account that the normal (transverse) velocity component u_y is set to zero and for the longitudinal velocity a free slip condition $\partial u_x / \partial y = 0$ is applied**.**

The initial condition at the beginning of the computational process (t = 0) was dry VSF. For all simulations it was assumed that the inflow discharge Q increases linearly from 0 to 600 l/s in 60 s. Then the inflow discharge was kept constant until steady state flow conditions were reached throughout the fishway.

Computational parameters

To ensure numerical stability and convergence, the time step was set at Δt = 0.1 s. For the majority of runs relatively good results were obtained already at Δt = 1 to 2 s, but due to consistency a unified time step was used for all simulations. Within one time step, a limit of maximum 50 to 1,000 iterations was set depending on the prescribed accuracy of the results, numerical mesh size and turbulence model used. Permissible relative error in continuity was set at 1% of total discharge Q = 600 l/s. Although the simulation reached a virtually steady state after about 1200 s, all runs were calculated to the final time of 3600 s.

Turbulence models

For flows with large swirling zones which occur in VSF, proper modeling of turbulence is extremely important in order to correctly calculate the hydrodynamic parameters of the flow. In this study three turbulence models were used (model with constant value of eddy viscosity v_T, the Smagorinsky turbulence model and the $k - \varepsilon$ turbulence model).

Model with constant value of eddy viscosity v_T

This model predicts that eddy viscosity is constant for the entire computational domain. Constant value of v_T was set as the average value of v_T in the third pool calculated with the $k - \varepsilon$ model. Constant eddy viscosity model generally gives satisfactory results for flow simulations of large water bodies where turbulent terms in dynamic Eq. (2) and (3) are not very important. For simulations of flows with large swirling zones, or when pollutant spreading is calculated, it is necessary to use a turbulence model that also accounts for turbulent transport processes in detail.

Smagorinsky turbulence model

In 1963, Smagorinsky introduced a turbulence model that assumes that Reynolds stresses τ_{ij} follow a gradient-diffusion process similar to molecular motion. Consequently, τ_{ij} is given by:

$$\tau_{ij} = -2\nu_T S_{ij}\,, \tag{4}$$

where S_{ij} is a strain rate tensor given by (in a 2-D depth averaged model, where i and j correspond to x and y directions):

$$S_{ij} = S_{xy} = \frac{1}{2}\left(\frac{\partial u_x}{\partial y} + \frac{\partial u_y}{\partial x}\right), \tag{5}$$

Smagorinsky eddy viscosity is then calculated as:

$$\nu_T = (C_S \Delta)^2 \sqrt{2 S_{xy} S_{xy}}\,, \tag{6}$$

where the filter width Δ is given by

$$\Delta = \sqrt{\Delta x \Delta y}\,. \tag{7}$$

C_s is the Smagorinsky coefficient which varies from flow to flow. Smagorinsky turbulence model is commonly used in large eddy simulations as a subgrid scale (SGS) model. In such cases, its value usually lies between $0.10 < C_s < 0.24$ (Rogallo and Moin, 1984).

As already pointed out by Kim (2001), other than for SGS modeling, there has been no systematic analysis to determine the Smagorinsky parameter. For simulations of VSF, the commonly used value of C_s = 0.17 gave inappropriate results. Calculated eddy viscosity was several orders of magnitude smaller compared to the eddy viscosity calculated by the $k - \varepsilon$ model. Consequently, the value of the Smagorinsky coefficient C_s was systematically varied until an average eddy viscosity in the central pool was achieved that was the same as obtained with the $k - \varepsilon$ model. As already pointed out by Mellor (2004) the simulations for both the $k - \varepsilon$ and the Smagorinsky model proved that eddy viscosity decreases with a finer numerical mesh. It follows from Eq. (6) that to keep a constant value of eddy viscosity v_T, a higher value of C_s has to be set when a finer numerical mesh is used (Fang, 2011). The present simulations confirmed this observation. A detailed examination of the influence of the Smagorinsky coefficient C_s on the individual flow case and the numerical grid will be the focus of further work.

The most important advantage of the Smagorinsky model is its simplicity and computational stability since it contains only one variable parameter. In addition, the model produces sufficient diffusion and dissipation to stabilize the numerical computations (Wilcox, 1994).

k – ε turbulence model

Rastogi and Rodi (1978) proposed the $k - \varepsilon$ model for shallow water flows. The equations of this model are given by:

$$\frac{\partial(hk)}{\partial t}+\frac{\partial(hu_x k)}{\partial x}+\frac{\partial(hu_y k)}{\partial y}=\frac{\partial}{\partial x}\left[h\left(\nu+\frac{\nu_T}{\sigma_k}\right)\frac{\partial k}{\partial x}\right]+$$
$$+\frac{\partial}{\partial y}\left[h\left(\nu+\frac{\nu_T}{\sigma_k}\right)\frac{\partial k}{\partial y}\right]+hP_k-C_D h\varepsilon+hP_{kv}, \quad (8)$$

$$\frac{\partial(h\varepsilon)}{\partial t}+\frac{\partial(hu_x \varepsilon)}{\partial x}+\frac{\partial(hu_y \varepsilon)}{\partial y}=\frac{\partial}{\partial x}\left[h\left(\nu+\frac{\nu_T}{\sigma_\varepsilon}\right)\frac{\partial \varepsilon}{\partial x}\right]+$$
$$+\frac{\partial}{\partial y}\left[h\left(\nu+\frac{\nu_T}{\sigma_\varepsilon}\right)\frac{\partial \varepsilon}{\partial y}\right]+hC_{1\varepsilon}\frac{\varepsilon}{k}P_k-C_{2\varepsilon}\frac{\varepsilon^2}{k}h+hP_{\varepsilon v}, \quad (9)$$

$$\nu_T=C_\mu\frac{k^2}{\varepsilon} \qquad P_k=\nu_T\left[2\left(\frac{\partial u_x}{\partial x}\right)^2+2\left(\frac{\partial u_y}{\partial y}\right)^2+\left(\frac{\partial u_x}{\partial y}+\frac{\partial u_y}{\partial x}\right)^2\right], \quad (10)$$

$$P_{kv}=C_k\frac{\mu_f^3}{h} \qquad C_k=\frac{1}{C_f^{1/2}}, \quad (11)$$

$$P_{\varepsilon v}=C_\varepsilon\frac{\mu_f^4}{h^2} \qquad C_\varepsilon=\frac{C_{\varepsilon r}C_{2\varepsilon}C_\mu^{1/2}}{C_f^{3/4}} \qquad C_f=\frac{n_g^2 g}{h^{1/3}}, \quad (12)$$

$$C_D=1.0; \quad C_{\varepsilon r}=3.6; \quad C_\mu=0.09; \quad C_{1\varepsilon}=1.44; \quad C_{2\varepsilon}=1.92;$$
$$\sigma_k=1.0; \quad \sigma_\varepsilon=1.31, \quad (13)$$

where k is turbulent kinetic energy per unit mass; ε is dissipation rate per unit mass; ν is kinematic viscosity of water and C_f is the bed friction coefficient. The term P_k accounts for the production of turbulent kinetic energy due to horizontal velocity gradients. The bed friction effect is included via the production terms P_{kv} and $P_{\varepsilon v}$.

The $k - \varepsilon$ turbulence model is the most widely tested and successfully applied model for a wide range of complex flows (Othman and Valentine, 2006). Although the results of these simulations are usually reasonably accurate, it is well known that in some cases the $k - \varepsilon$ model overpredicts the real production of turbulent kinetic energy when turbulence is non-isotropic, which happens near stagnation points (Bermúdez et al., 2010). For weak shear layers and axisymmetric jets some of the constants have to be replaced by functions (Rodi, 1993). Another problem of eddy viscosity models is that for large values of eddy viscosity, Boussinesq's assumption can imply negative normal Reynolds stresses which is physically incorrect (Cea et al., 2007; Chorda et al., 2010). In order to improve the results for such cases, different limiters have been proposed by Menter (1993) and Durbin (1996). Nevertheless, in the present study PCFLOW2D with the original $k - \varepsilon$ model by Rastogi and Rodi (1978) was used and it gave satisfactory results, as discussed below.

RESULTS AND DISCUSSION

Manning's roughness coefficient

Firstly, the influence of bed friction coefficient was examined. Runs with Manning's coefficients n_g = 0.01, 0.02 and 0.03 s/m$^{1/3}$ were performed. Fig. 3 shows the velocity at cross section IV. Results showed that significant differences occur only in the main flow region where the velocities with n_g = 0.02 and 0.03 s/m$^{1/3}$ were 2 to 3% and 4 to 7% lower, respectively, than with n_g = 0.01 s/m$^{1/3}$. These results differ slightly from those by Cea et al. (2007) who found no differences for Manning's coefficients ranging between n_g = 0 (no friction) and n_g = 0.03 s/m$^{1/3}$. The present study confirmed that bed friction does not play an important role for this type of flow. Finally, the Manning's coefficient n_g = 0.01 s/m$^{1/3}$ was selected according to the flume material.

Velocity field

So far different geometries of VSF with 5–15% longitudinal slope have been studied on scale models (Liu et al., 2006; Puertas et al., 2004; Rajaratnam et al., 1986; Rajaratnam et al., 1992; Tarrade et al., 2008), as well as with numerical programs (Bermúdez et al., 2010; Cea et al., 2007; Chorda et al., 2010; Violeau, 2012). The results of these studies showed that generally two flow patterns occur. Wu et al. (1999) described them as: ″In pattern 1, the flow from the slot travels through the center of the pool to the next slot with two large recirculation regions located on either side of the jet. In pattern 2, a significant part of the flow from the slot travels toward the sidewall in between the long baffles near the bed and a part of this flow travels to the next slot near the bed, whereas the rest rises to the water surface and then travels to the next slot. A large recirculation region is formed on the other side of this jet (between the short baffles) with another smaller recirculation region with a horizontal axis of rotation located near the long baffle″ (Wu et al., 1999, p. 352). Flow pattern 1 occurred for smaller slopes and flow pattern 2 for larger slopes according to previous studies. Fig. 4 shows velocity vectors in the central pool of the VSF. To improve clarity, velocity vectors are not plotted in all computational cells.

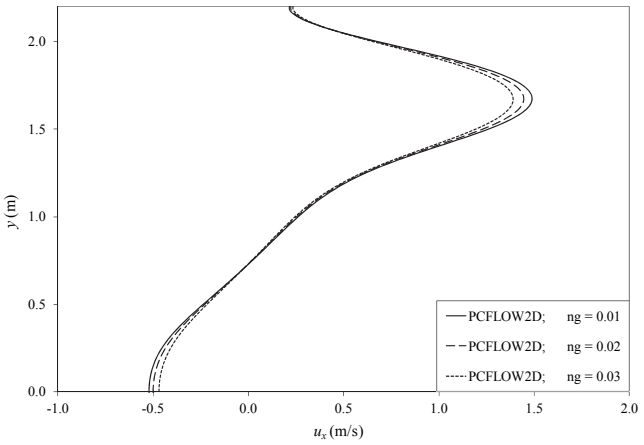

Fig. 3. Longitudinal velocity u_x (m/s) at cross section IV for various n_g.

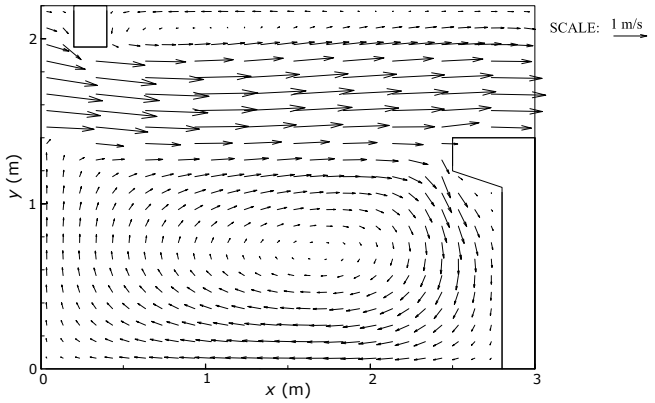

Fig. 4. Velocity field in the central pool of VSF Blanca. v_T = const. = 0.007324 m^2/s; mesh 1 × 1 cm; Δt = 0.1 s.

As expected, due to a small longitudinal slope S_0 = 1.67%, pattern 1 occurred in the case of VSF Blanca (Fig. 4). This pattern was also confirmed by observations on the physical model. Because of relatively short baffles, only a subtle recirculating zone appeared between them. A much more significant recirculating zone covered the entire area between long baffles with its center at about x = 1.78 m and y = 0.73 m. In the slot region maximum velocities of around 1.7 m/s for the prototype were calculated.

Sensitivity analysis of the numerical mesh

Three different mesh sizes were tested in order to assure mesh-independent results (Table 1). The mesh-size sensitivity analysis was performed for all three turbulence models used.

Table 1. Characteristics of numerical meshes used for mathematical modeling.

Mesh No.	Cell size ($\Delta x \times \Delta y$)	Number of cells ($N_x \times N_y$)
M1	5.0 × 5.0 cm	620 × 46 = 28 520
M2	2.5 × 2.5 cm	1 238 × 90 = 111 420
M3	1.0 × 1.0 cm (3rd + ½ of 2nd and 4th pool) 5.0 × 1.0 cm (the rest)	1 116 × 222 = 247 752

It must be pointed out that the choice of numerical scheme affected the accuracy of the results. A first order upwind scheme, used at certain points as part of the hybrid scheme (where Pe > 2) in PCFLOW2D produces numerical diffusion which can be estimated as (Patankar, 1980):

$$\nu_{num} = \frac{V \Delta x \Delta y \left|\sin 2\alpha\right|}{4\left(\Delta y \left|\sin\alpha\right|^3 + \Delta x \left|\cos\alpha\right|^3\right)}. \quad (14)$$

It is evident from Eq. (14), where V denotes the magnitude of velocity and α the angle between velocity vector and the x axis, that the mesh size, given with Δx and Δy, has an important influence on the magnitude of numerical diffusion. The influence of numerical diffusion on the results can be estimated using the ratio between numerical diffusion and eddy viscosity coefficient v_T. In PCFLOW2D, this ratio is denoted VISRAT. For values VISRAT > 1, numerical diffusion plays a major role and the appropriate value of eddy viscosity v_T has little or no importance. Fig. 5 shows streamlines calculated with the $k - \varepsilon$ turbulence model for various cell sizes.

A coarse mesh (M1) gave very smooth results with a subtle recirculation zone in the lower-left corner of the pool (Fig. 5a). This was due to the numerical diffusion which artificially diminished recirculation in the pool. With a denser numerical mesh this recirculation zone increased (Fig. 5b and Fig. 5c). Results of VISRAT ratio for all three meshes for the $k - \varepsilon$ turbulence model are shown in Fig. 6.

With the finest mesh (M3), numerical diffusion had virtually no impact on the results. For the M3 mesh, the numerical diffusion represented less than 10% of the one calculated with the $k - \varepsilon$ model in 95% of the middle pool (Fig. 6c). Also, in only 1% of the pool, the numerical diffusion prevailed over the one calculated with the $k - \varepsilon$ model, i.e. VISRAT > 1. For this reason, all the following main simulation results of the present study were obtained with 1.0 by 1.0 cm numerical mesh.

Measured values were in relatively good agreement with simulations for all three mesh sizes (Fig. 7). Significant differences appeared at y < 1.20 where the simulation of the larger eddy differed considerably for runs with various cell sizes (Fig. 5).

Influence of turbulence models

In VSF, velocity fields determine whether or not the fish are able to pass from one pool to another, therefore the ability of a turbulence model to simulate and predict the flow pattern is of great importance. A turbulence model that calculates a level of turbulent energy that is too low predicts excessive velocities while excessive calculated turbulence levels result in predicted velocities that are too low (Cea et al., 2007). Turbulence levels can be given in terms of v_T values (Fig. 8).

As discussed previously in the section "turbulence models", a two-equation $k - \varepsilon$ model was the most accurate turbulence model in the present study. Thus the average eddy viscosity $\overline{v}_T$ in the observed pool calculated by the $k - \varepsilon$ model was applied for the constant viscosity model (v_T = 0.007324 m^2/s). The same applies for the Smagorinsky turbulence model. Smagorinsky constant C_s was determined iteratively until the same average eddy viscosity in the observed pool (C_s = 7.32) was obtained. As a result of similar values of v_T for all three turbulence models, a good correlation between simulated velocity fields was achieved (Fig. 9).

It should be pointed out that usually the relevant average value of the eddy viscosity coefficient v_T is not known so its determination is rather difficult. The same applies to the Smagorinsky model. When a common value of the Smagorinsky constant for SGS models (C_s = 0.17) (Kim, 2001; Rogallo and Moin, 1984; Wilcox, 1994) was used, the obtained values of v_T were significantly lower than those calculated with the $k - \varepsilon$ model. This resulted in increased velocity in the slot region and a different velocity field in the pool. With the Smagorinsky constant set to C_s = 7.32, better agreement between results was obtained (Fig. 9 and Fig. 10). While the size of the upper eddy between short baffles was practically the same for both the Smagorinsky and the $k - \varepsilon$ model, the constant viscosity model yielded a somewhat larger eddy. An important difference in results of the employed turbulence models was their ability to simulate a large recirculating zone between large baffle piers. Both the constant viscosity model and the Smagorinsky model yielded one single large eddy while the $k - \varepsilon$ model yielded an additional eddy rotating in the opposite direction in the lower-left (upstream) corner of the pool (Fig. 9). Such an eddy was also observed in the physical model.

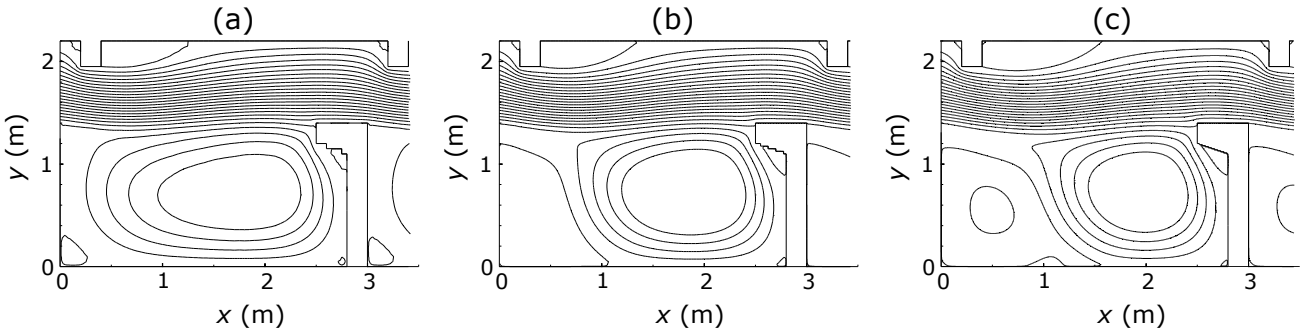

Fig. 5. Streamlines calculated with the $k - \varepsilon$ turbulence model for various cell sizes. (a) 5.0 × 5.0 cm cells, (b) 2.5 × 2.5 cm cells, (c) 1.0 × 1.0 cm cells.

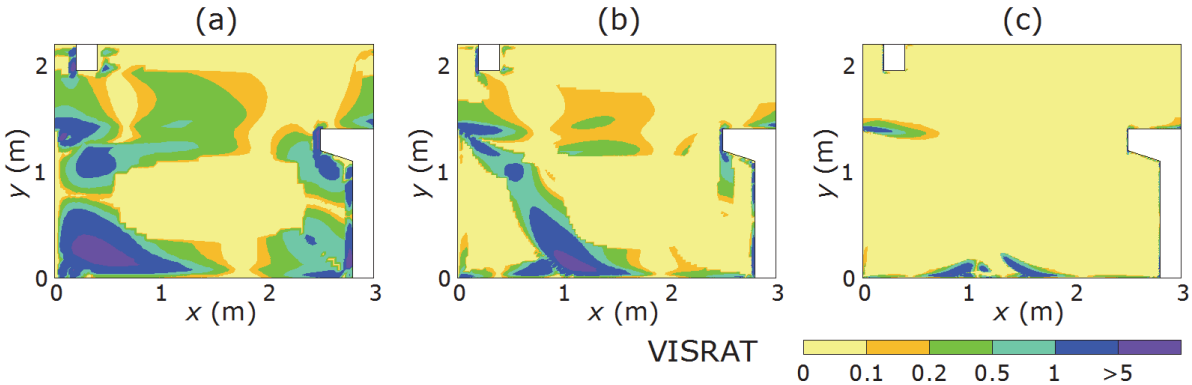

Fig. 6. Values of the ratio between numerical diffusion and eddy viscosity coefficient ν_T for the $k - \varepsilon$ turbulence model (i.e. VISRAT values). (a) 5.0 × 5.0 cm cells, (b) 2.5 × 2.5 cm cells, (c) 1.0 × 1.0 cm cells.

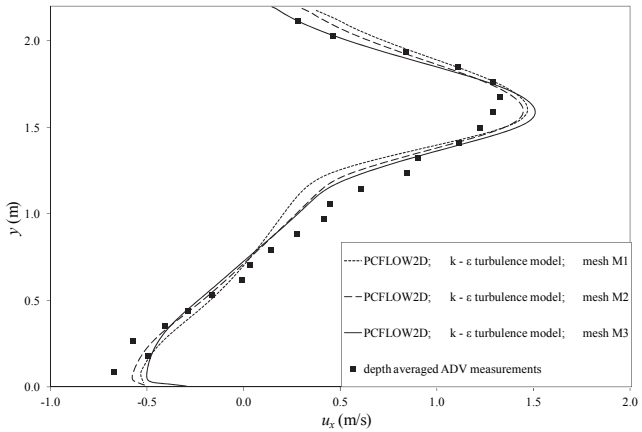

Fig. 7. Longitudinal velocity u_x (m/s) at cross section III.

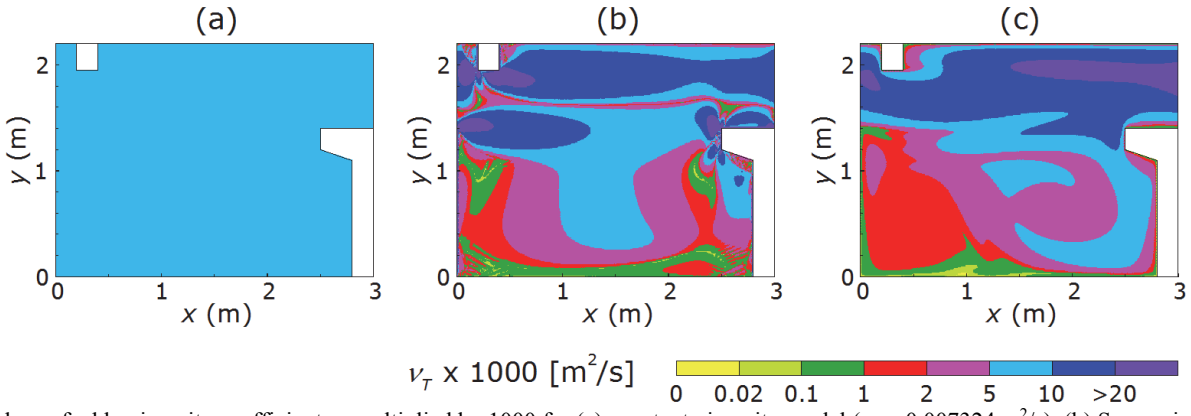

Fig. 8. Values of eddy viscosity coefficient ν_T multiplied by 1000 for (a) constant viscosity model (ν_T = 0.007324 m^2/s), (b) Smagorinsky model (C_s = 7.32) and (c) $k - \varepsilon$ model. In all cases 1 × 1 cm mesh is used.

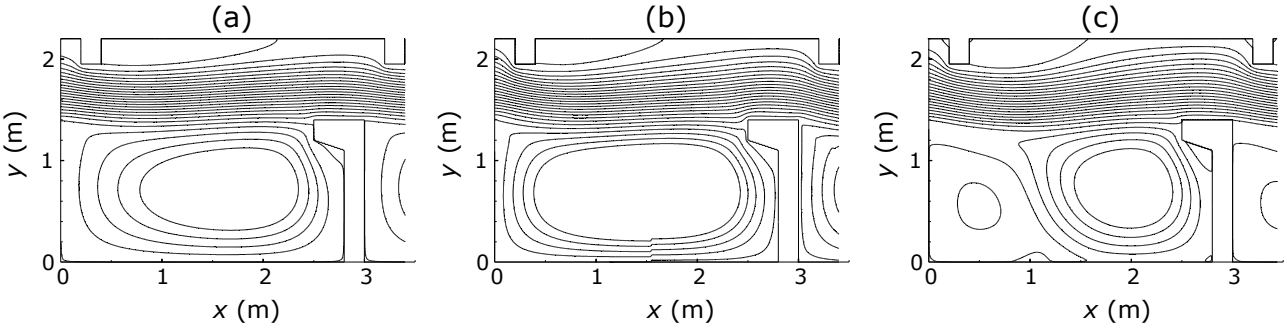

Fig. 9. Streamlines for (a) constant viscosity model (v_T = 0.007324 m^2/s), (b) Smagorinsky model (C_s = 7.32) and (c) $k - \varepsilon$ model. In all cases 1 × 1 cm mesh is used.

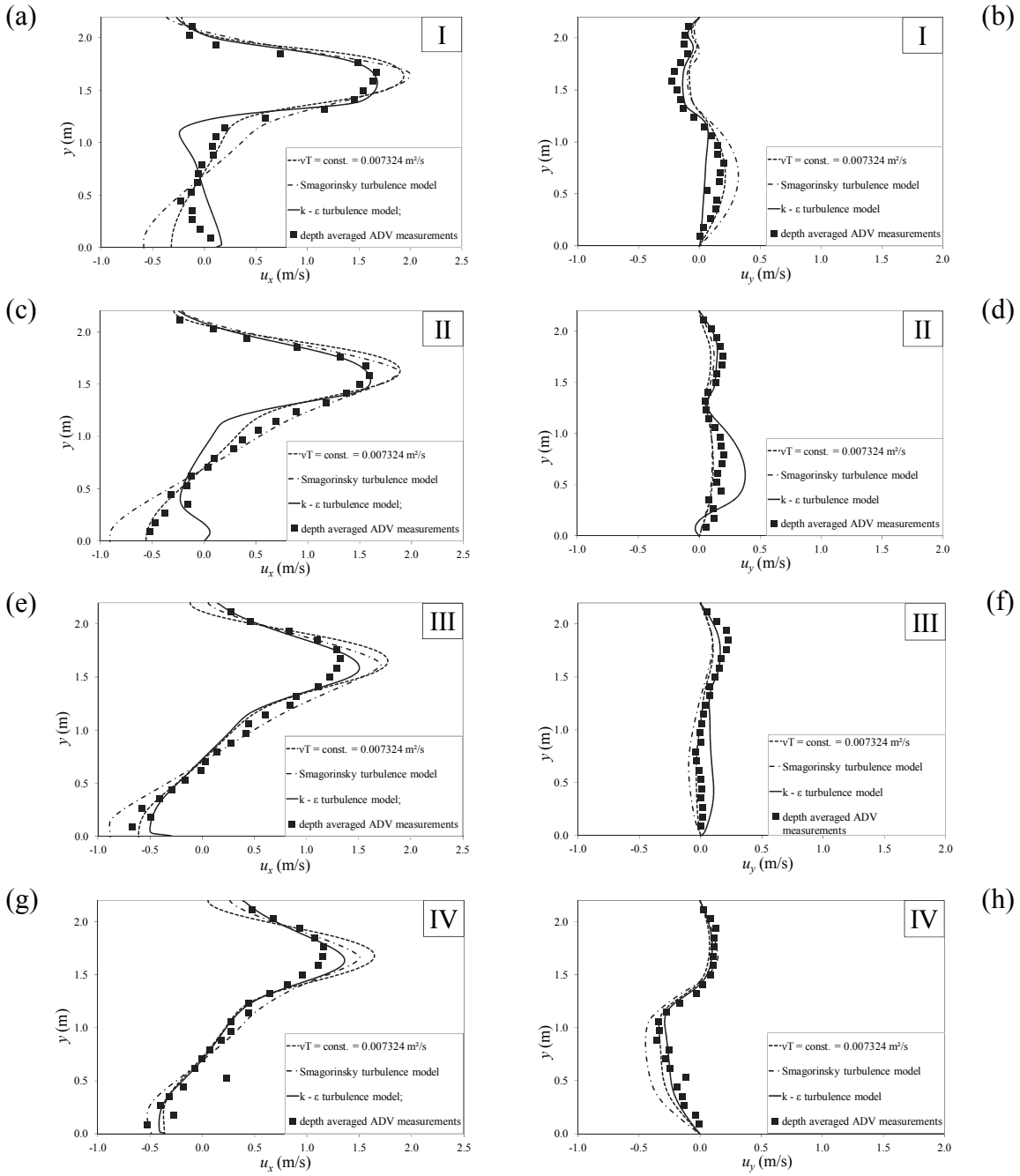

Fig. 10. (a), (c), (e), (g) calculated and measured depth averaged velocity component u_x at cross sections I, II, III and IV; and (b), (d), (f), (h) calculated and measured depth averaged velocity component u_y at cross sections I, II, III and IV.

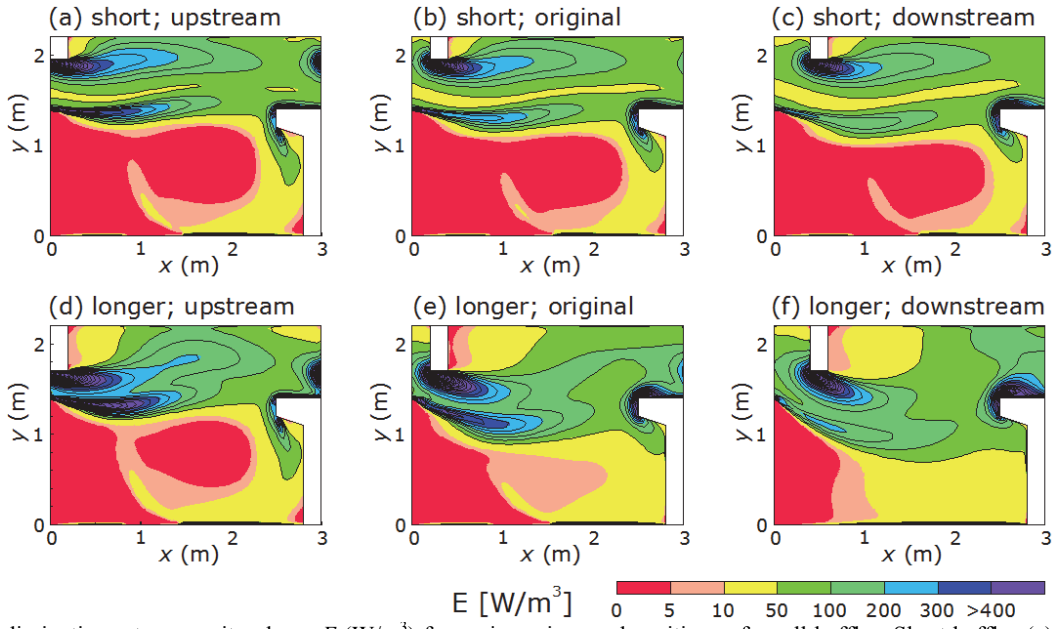

Fig. 11. Energy dissipation rate per unit volume E (W/m^3) for various sizes and positions of small baffles. Short baffles (a) to (c); longer baffles (d) to (f).

Velocity profiles in Fig. 10 show small differences between the calculated results with different turbulence models. One of the most important features of the flow in VSF is its maximum longitudinal velocity in the slot region. The constant eddy viscosity and Smagorinsky models yielded slightly higher longitudinal velocities u_x than the $k - \varepsilon$ model. Comparison of calculated and measured values (Fig. 10) showed that velocities from the $k - \varepsilon$ model were in accordance with results of ADV measurements.

It can be concluded that the differences between the results of the turbulence models used were not significant. This was due to a good choice of eddy viscosity v_T and Smagorinsky coefficient C_s which in practice are usually very difficult to obtain. However, the $k - \varepsilon$ model gave more accurate results and was used in subsequent calculations.

Application to fishway analysis

Numerical simulations for six pool geometries (different positions and sizes of small baffle piers) were carried out. Positions of short baffle piers were x = 0.0 m, 0.2 m and 0.4 m with x = 0.2 m being the original one. Original length of baffle piers was d_y = 0.25 m and the alternative length was double its size d_y = 0.50 m. All simulations were carried out with the same boundary conditions (Q = 600 l/s, h_{out} = 0.88 m) and with the same numerical parameters (Δt = 0.1 s, etc.) as described previously in sections "boundary and initial conditions" and "computational parameters". The focus of the present study was primarily on comparing the maximum velocity in the pool and the energy dissipation rate since these determine whether or not fish are able to migrate through the VSF.

The average energy dissipation rate per unit volume P_V in the pools is usually calculated using a simple formula. Lower values are generally preferred. For fishways designed for riverine species, such as VSF Blanca, the average energy dissipation rate per unit volume P_V of less than 150 W/m^3 is advisable (Larinier, 2002). However, detailed determination of spatial distribution of the energy dissipation rate is of great importance for better evaluation of fish ability to pass through the VSF (Chodra et al., 2010). Fig. 11 shows spatial distribution of energy dissipation rate per unit volume E (W/m^3), calculated as $\rho \times \varepsilon$, for various sizes and positions of small baffles.

All three variants with short baffles gave similar results with the trend of energy dissipation rate values decreasing with piers positioned more downstream. Major differences occurred with the installation of longer baffles since the energy dissipation in all three variants increased in relation to short baffles. Comparison of variants with longer baffles also indicated the trend of energy dissipation rate values decreasing with piers positioned more downstream. Variant (c) had the lowest energy dissipation rate and is thus the best option according to criteria given by Larinier (2002).

As already mentioned, maximum flow velocities occur in the slot region of a pool. For different variants calculated maximum velocities varied between 1.501 and 1.872 m/s. Comparison of maximum flow velocities in the pool confirmed the choice of the variant (c) with downstream position of original sized baffle piers as the most suitable one (Table 2).

Table 2. Comparison of maximum velocities u_{max} (m/s) and energy dissipation rate per unit volume E (W/m^3) for various sizes and positions of small baffles.

Baffle size and position	b_0 (m)	u_{max} (m/s)	E (W/m^3)	E < 200 (W/m^3)	E < 150 (W/m^3)	E < 100 (W/m^3)	E < 50 (W/m^3)
short; upstream	0.550	1.792	82	92%	87%	78%	58%
short; original	0.585	1.700	76	94%	89%	79%	58%
short; downstream	0.680	1.615	69	96%	91%	82%	59%
longer; upstream	0.300	1.872	101	89%	82%	72%	59%
longer; original	0.361	1.672	93	90%	84%	71%	53%
longer; downstream	0.500	1.501	90	93%	87%	71%	49%

CONCLUSIONS

Good agreement between measurements on a scaled physical model and results from the numerical model PCFLOW2D was found. It was confirmed that when calculating flows with distinct eddies (as is the case in VSF) it is crucial to use a turbulence model that correctly takes into account production and dissipation of turbulent energy. It was found that the constant eddy viscosity model within PCFLOW2D was not completely appropriate for calculating flow in VSF. The same can be concluded about the zero-equation Smagorinsky model. The main weakness of both models is the difficulty of determining their necessary coefficients. Satisfactory results were obtained with the employment of the $k - \varepsilon$ model which predicted velocity fields that were in accordance with ADV measurements.

When calculating flows with high levels of turbulence, it is of great importance to take into account the effect of numerical diffusion. With first order numerical scheme in PCFLOW2D, a sufficiently fine numerical mesh had to be employed to eliminate its influence on the results.

Simulations of variant configurations of VSF Blanca showed that even small changes in geometry produce more fish-friendly flow characteristics in pools. This knowledge should be taken into account in designing future VSF´s. The EU Water Framework Directive dictates the construction of fish passages and the present study shows that PCFLOW2D program is an appropriate tool to meet the main demands of the VSF design.

List of notations

b_0 = slot width [m]
C_s = Smagorinsky coefficient [–]
d_x = short baffle pier width [m]
d_y = short baffle pier length [m]
E = energy dissipation rate per unit volume [W/m^3]
g = gravity acceleration [m/s^2]
h = water depth [m]
h_{out} = outlet boundary condition [m]
k = turbulent kinetic energy per unit mass [m^2/s^2]
L = pool length [m]
n_g = Manning's roughness coefficient [s/m$^{1/3}$]
N_x = number of numerical cells in streamwise direction [m]
N_y = number of numerical cells in transverse direction [m]
Pe = Peclet number [–]
P_V = average energy dissipation rate per unit volume [W/m^3]
Q = discharge [m^3/s]
S_0 = longitudinal slope [–]
S_{ij} = rate of strain tensor [s^{-1}]
u_{max} = depth averaged maximum velocity [m/s]
u_x = depth averaged streamwise velocity component [m/s]
u_y = depth averaged transverse velocity component [m/s]
U_x = streamwise velocity component [m/s]
U_y = transverse velocity component [m/s]
W = pool width [m]
x = streamvise coordinate [m]
y = transverse coordinate [m]
z = vertical coordinate [m]
z_b = bed elevation level [m.a.s.l.]
Δ = filter width [m]
Δt = time step [s]
Δx = cell size in streamwise direction [m]
Δy = cell size in transverse direction [m]
ε = dissipation rate per unit mass [m^2/s^3]
v = kinematic viscosity of water [m^2/s]
v_{num} = numerical diffusion [m^2/s]
v_T = kinematic coefficient of eddy viscosity [m^2/s]
ρ = density of water [kg/m^3]
τ_{ij} = Reynolds stresses [m^2/s^2]

REFERENCES

Bermúdez, M., Puertas, J., Cea, L., Pena, L., Balairón, L., 2010. Influence of pool geometry on the biological efficiency of vertical slot fishways. Ecological Engineering, 36, 10, 1355–1364.

Cea, L., Pena, L., Puertas, J., Vazquez-Cendon, M.E., Pena, E., 2007. Application of several depth-averaged turbulence models to simulate flow in vertical slot fishways. J. Hydraulic Eng., 133, 2, 160–172.

Chorda, J., Maubourguet, M.M., Roux, H., George, J., Larinier, M., Tarrade, L., David, L., 2010. Two-dimensional free surface flow numerical model for vertical slot fishways. J. Hydraulic Res., 48, 2, 141–151.

Clay, C.H., 1995. Design of Fishways and Other Fish Facilities. Dept. of Fisheries of Canada, Ottawa, Canada.

Četina, M., 1988. Mathematical modeling of two-dimensional turbulent flows. Acta Hydrotechnica, 6, 5, 1–56. (in Slovenian with extended abstract in English.)

Četina, M., 2000. Two-dimensional modeling of free surface flow. Acta Hydrotechnica, 18, 29, 23–37.

Četina, M., Rajar, R., Hojnik, T., Zakrajšek, M., Krzyk, M., Mikoš, M., 2006. Case study: Numerical simulations of debris flow below Stože, Slovenia. J. Hydraulic Eng., 132, 2, 121–130.

Durbin, P., 1996. On the k - ε stagnation point anomaly. Int. J. Heat Fluid Flow, 17, 1, 89–90.

Enders, E.C., Boisclair, D., Roy, A.G., 2003. The effect of turbulence on the cost of swimming for juvenile Atlantic salmon. Can. J. Fish. Aquat. Sci., 60, 9, 1149–1160.

Fang, L., 2011. A new dynamic formula for determing the coefficient of Smagorinsky model. Theor. Appl. Mech. Lett., 1, 3, Available at http://taml.aip.org/resource/1/tamlbx/v1/i3/p032002

Hamzić, R., 2012. Upgrade of PCFLOW2D model with k – ε turbulence model for unsteady flow. B. Sc. thesis, Faculty of Civil and Geodetic Engineering, University of Ljubljana, Slovenia. (in Slovenian.)

HESS, d.o.o., 2010. Passage for aquatic organisms on HPP Blanca. Available at http://www.he-ss.si/pdf/kratek-opis.pdf (in Slovenian.)

Josipovič, Z., Ciuha, D., 2009. Passage for aquatic organisms on HPP Blanca. As-built design documentation, IBE, d.d, Ljubljana. (in Slovenian.)

Kim, T.K., 2001. A Modified Smagorinsky Subgrid Scale Model for the Large Eddy Simulation of Turbulent Flow. PhD thesis., Univeristy of California, Davis, USA. Available at http://arxiv.org/abs/math/0209377.

Kolman, G., Mikoš, M., Povž, M., 2010. Fish passages on hydroelectric power dams in Slovenia. Nature conservation, 24, 85–96. Available at http://www.zrsvn.si/dokumenti/63/2/2010/Kolman_Mikos_povz_2227.pdf (in Slovenian.)

Larinier, M., 2002. Pool fishways, pre-barrages and natural bypass channels. In: Larinier, M., Travade, F., Porcher, J.P. (Eds.): Fishways: biological basis, design citeria and monitoring, pp. 364 suppl., pp. 54–82.

Liu, M., Rajaratnam, N., Zhu, D.Z., 2006. Mean flow and turbulence structure in vertical slot fishways. J. Hydraulic Eng., 132, 8, 765–777.

Mellor, G.L., 2004. User guide for a three-dimensional, primitive equation, numerical ocean model. Program in Atmos-

pheric and Oceanic Sciences, Princeton University. Available at http://www.aos.princeton.edu/WWWPUBLIC/htdocs.pom/FTPbackup/usersguide0604.pdf

Menter, F.R., 1993. Zonal two-equation k - ω turbulence models for aerodynamic flows. AIAA paper 93–2906. 24th Fluid Dynamics Conf., Orlando, Florida, USA.

Othman, F., Valentine, E.M., 2006. Numerical modelling of the velocity distribution in a compound channel. J. Hydrol. Hydromech., 54, 3, 269–279.

Patankar, S.V., 1980. Numerical Heat Transfer and Fluid Flow. McGraw-Hill Book Company, New York, USA.

Pena, L., Cea, L., Puertas, J., 2004. Turbulent flow: An experimental analysis in vertical slot fishways. IAHR, 5th Int. Symp. on Ecohydraulics Madrid, Spain, pp. 881–888.

Powers, P., Orsborn, J., 1984. New concepts in fish ladder design: Analysis of barriers to upstream fish migration. Volume IV of IV: Investigation of the physical and biological conditions affecting fish passage success at culverts and waterfalls. Final Rep. 1982–1984. BPA Rep. DOE/BP-36523-1 Project No. 198201400, Bonneville Power Administration.

Puertas, J., Pena, L., Teijeiro, T., 2004. Experimental approach to the hydraulics of vertical slot fishways. J. Hydraulic Eng., 130, 1, 10–23.

Rajaratnam, N., Van der Vinne, G., Katopodis, C., 1986. Hydraulics of vertical slot fishways. J. Hydraulic Eng., 112, 10, 909–927.

Rajaratnam, N., Katopodis, C., Solanki, S., 1992. New designs for vertical slot fishways. Can. J. Civil Eng., 19, 3, 402–414.

Rastogi, A.K., Rodi, W., 1978. Predictions of heat and mass transfer in open channels. J. Hydraulic Div., 104, 3, 397–420.

Rodi, W., 1993. Turbulence Models and Their Application in Hydraulics – A State-of-the-Art Review. Institut fur Hydromechanik, University of Karlsruhe, Karlsruhe, Germany.

Rogallo, R.S., Moin, P., 1984. Numerical simulation of turbulent flows. Ann. Rev. Fluid Mech., 16, 99–137.

Smagorinsky, J., 1963. General circulation experiments with the primitive equations. Mon. Wea. Rev., 91, 3, 99–164. Available at http://docs.lib.noaa.gov/rescue/mwr/091/mwr-091-03-0099.pdf

Tarrade, L., Texier, A., David, L., Larinier, M., 2008. Topologies and measurements of turbulent flow in vertical slot fishways. Hydrobiol., 609, 177–188.

Valentine, E.M., Zulfiqar, A., Swailes, D.C., 2002. A two-zone model for longitudinal dispersion in chennels with idealized pools and riffles. J. Hydrol. Hydromech., 50, 2, 77–103.

Violeau, D., 2012. Fluid Mechanics and the SPH Method: Theory and Applications. First Edition, Oxford, United Kingdom.

Wilcox, D.C., 1994. Turbulence Modeling for CFD. DCW Industies, California, USA.

Wu, S., Rajaratnam, N., Katopodis, C., 1999. Structure of flow in vertical slot fishway. J. Hydraulic Eng., 125, 4, 351–360.

Received 11 June 2013
Accepted 15 January 2014